Rasayely
Membrane Science International
https://rasayely-journals.com/index.php/msi
Vol 1(1); 12–23, 2022

RASAYELY

Original Article Open Access

Study on Fouling Mechanisms of Homogeneous Ion-Exchange Membranes during Removal of Soluble Saccharides from the Aqueous Solution Containing Ionic Liquids by Electrodialysis

Hongxiang Xu[1], Weichao Li[1,4], Junfeng Wang[2,3,4,*], Wentao Li[1,4], Shanshan Zhang[2,4], Yi Nie[2,3,4], Daoguang Wang[2,3,4]

[1]*School of Chemical and Environmental Engineering, China University of Mining and Technology (Beijing), Beijing 100083, China*

[2]*State Key Laboratory of Multiphase Complex Systems, Institute of Process Engineering, Chinese Academy of Sciences, Beijing 100190, China*

[3]*Innovation Academy for Green Manufacture, Chinese Academy of Sciences, Beijing 100190, China*

[4]*Beijing Key Laboratory of Ionic Liquids Clean Process, Chinese Academy of Sciences, Beijing 100190, China*

[*]Author to whom any correspondence should be addressed; e-mail: junfwang@ipe.ac.cn, Tel.: +86 10 82544875. Fax: +86 10 82544875

Received 29 December 2021; Revised 01 March 2022; Accepted 10 March 2022; Published 29 April 2022

Academic Editor: Alberto Figoli, Institute on Membrane Technology, ITM-CNR, Rende, Italy

Abstract

Electrodialysis (ED) method showed an effective separation ability of soluble saccharides from the ionic liquid (IL) aqueous solution confirmed by our previous work. This paper focused on the fouling mechanisms of ion exchange membranes (IEMs), i.e., the cation exchange membrane (CEM) and the anion exchange membrane (AEM). Firstly, the effects of operation time, IL concentration, glucose concentration, and temperature of dilute solution on membrane fouling were investigated. Results indicated that the low IL concentration also resulted in the fouling of the IEMs. The addition of glucose had a slight effect on the AEMs, but a serious effect on the CEM. The effect of temperature on the IEM fouling was the most significant, Over the temperature range from 25 to 40 °C, the ion exchange capacity (IEC) of CEMs and AEMs decreased from 0.5370 mol/kg and 0.4565 mol/kg to 0.4171 mol/kg and 0.3172 mol/kg, respectively. Subsequently, the characteristic results showed that the surface hydrophobicity of the IEMs decreased due to the adsorption of the hydrophilic components, i.e., anions and cations of ILs. The IEM fouling during the ED process for the separation of glucoses from the IL aqueous solution was mainly caused by the adsorption of the ILs through the electrostatic interactions. Glucoses was easier to be enriched on the surface of the CEMs, which could promote the cluster behavior of the ILs and then block the membrane pores or interlayers, thus increasing the irreversible fouling of CEM. In addition, compared to the other cleaning solution, the HCl solution showed a good cleaning effect for the fouled IEMs. Under the optimized conditions, the performance of the fouled CEMs could be recovered to 94.57% of the pristine membrane, and that of the fouled AEMs could be recovered to the pristine membrane level by a long cleaning process.

Keywords

Ionic liquids; electrodialysis; membrane fouling mechanisms; Soluble saccharides

1. Introduction

Ionic liquids (ILs) are one of the best "green solvents" available, in the cellulose dissolution field that has gained considerable attention [1–6]. Especially, the solvent 1-ethyl-3-methylimidazolium diethylphosphate ([Emim]Dep) has been shown to be an effective cellulose dissolving and

regeneration agent [7–10]. However, during the steps of draft and water washing for the dissolution process of cellulose with IL as the solvent, a substantial volume of IL aqueous solution containing the cellulose hydrolyzed products, i.e., soluble saccharides, was produced. To achieve the recycling and reuse of ILs, it is desirable to develop a method for separating soluble saccharides from IL aqueous solution that is both effective and environmentally friendly. Our previous work testified that the Electrodialysis (ED) method could effectively separate the organic compounds which were generated during the process of cellulose regeneration with the IL as a solvent, from the IL aqueous solution. The removal efficiency of soluble saccharides was up to 98.11% under optimal conditions [11]. To further obtain the optimized parameters for the ED method, it is necessary to investigate the mechanisms of membrane fouling, and then establish the effective cleaning method of the fouled IEMs.

One of the most serious difficulties in the operation of the electrodialysis desalination process is fouling of the ion exchange membrane (IEM) [12–15]. Membrane fouling is essentially caused by the adsorption of foulants on the membrane surface or the blockage of foulants inside the IEM pores, resulting in the increase of the membrane resistance and the decrease of the ion exchange capacity (IEC) [16–20]. The characteristics and mechanisms of membrane fouling caused by the different types of components are also different. Therefore, different methods can be used to reduce the occurrence of IEM fouling. Usually, the prevention and control measures of the IEM fouling during the ED process include the pretreatment of raw materials [21,22], the optimization of operating conditions [23,24], the modification of ion exchange membrane [25,26], and the membrane cleaning process [27,28]. Among these methods, the membrane cleaning method is relatively simple, and it is possible to overcome the shortcomings of multi-type fouling adaptability. Generally, water, alkali, acid, and surfactants solutions are often used as the cleaning solutions for membrane fouling [29].

The main objective of the research is to investigate fouling of homogenous IEM during the ED process for removing glucose from an aqueous solution containing ILs formed during the cellulose dissolving process using [Emim]Dep IL as the solvent. The impact of operational factors such as operating time, initial [Emim]Dep concentration in the feed solution, initial glucose concentration in the feed solution, and temperature on IEC and IEM contact angle was first examined. The cleaning effect of different cleaning solutions on the fouled IEM was investigated, in order to select suitable cleaning solutions. The properties of the fouled IEM were characterized by Fourier transform infrared spectroscopy (FT-IR), X-ray photoelectron spectroscopy (XPS), elementary analysis, and scanning electron microscopy-energy dispersive X-ray spectroscopy (SEM-EDS) to further study the fouling mechanism. Finally, the fouling mechanism model of IEM in the process of removing glucose from the aqueous solution containing ILs by the ED method was proposed.

2. Experimental

2.1. Materials

All the reagents within the analytical grade were used as received while not more purification. Glucose and hydrochloric acid (HCl) were purchased from Sinopharm Chemical Reagent Co., Ltd (China). Sodium hydroxide (NaOH), phenolphthalein, and methyl orange were obtained from McLin Biochemical Technology Co., Ltd (China). 1-ethyl-3-methylimidazolium diethylphosphate ([Emim] Dep) was synthesized in our laboratory in step with the strategy taken from the literature [21]. [Emim]Dep was characterized by ^{1}H and ^{13}C NMR, and the characterization results were shown in Supporting Information Figure S1 and Figure S2, respectively. In this work, to avoid the introduction of other ions, the aqueous solution containing 40 g/L [Emim] Dep was used as the electrode solution [11]. High-purity Milli-Q water (resistivity > 18.2 MΩ·cm and conductivity < 0.1 $\mu S \cdot cm^{-1}$) was used to prepare all aqueous solutions.

2.2. Experimental Set-Up

ED apparatus was provided by Hefei ChemJoy Polymer Materials Co., Ltd (China). The membrane fouling experiments were carried out in a five-compartment ED stack with two homogeneous CEMs (CJMC-3, Hefei ChemJoy Polymer Materials Co., China) and one homogeneous AEM (CJMA-3, Hefei ChemJoy Polymer Materials Co., China) as shown in **Figure 1**. The CEM with functional sulfonic groups and the AEM with functional quaternary ammonium were composed of styrene-divinylbenzene co-polymer. The parameters of the ion-exchange membranes are shown in **Table 1**. The effective area of each membrane was 189 cm^2. The neighboring membranes were separated by a spacer with a thickness of 0.8 mm. The solution temperature was controlled by a thermostat ET-3030 (Shenzhen Bangqichuangyuan Technology Co., China). All of the compartments in the ED set-up were flushed with distilled water before each experiment.

2.3. Membrane Fouling Experiments

The membrane fouling experiments were carried out in an ED apparatus, as shown in **Figure 1**. The membrane stack with two CEMs and one AEM which were alternately arranged between the cathode and anode was divided into the dilute compartment (DCT), the concentrated compartment (CCT), and the electrode compartment (ECT). The CCT was filled with 2 L deionized water. The DCT, in which the initial solution was 2 L mixed solution containing IL and glucose, i.e. the feed solution. To avoid the introduction of other ions, such as Na^+ and SO_4^{2-}, 1 L of 40 g/L [Emim]Dep aqueous solution was used as the electrode rinse solution. The solutions in the three vessels were circulated through the DCT, CCT, and ECT, respectively, and then flowed into the three vessels. For all experiments, the corresponding magnetic drive pump circulated three types of solutions at a flow rate of 40 L/h. Each fouling experiment with the same type of IEM was conducted three times, with the average of the three measurements used to determine the characterization result. The utilized IEM was cleaned with ultrapure water after each test and then air-dried for further characterization.

Table 1: Physical and chemical properties of ion-exchange membranes.

Properties	Indexes	
	AM	CM
Thickness in dry state (μm)	140-160	180-210
Ion-exchange capacity (meg/g)	0.5-0.6	0.8-1.0
Water content (%)	15-20	40-50
Burst strength (MPa)	>0.35	>0.35
Resistance of surface (Ω·cm^2)	3.5-4.5	2.5-3.5
Permselectivity (%)	>93	>93
Temperature tolerance (°C)	<40	<40

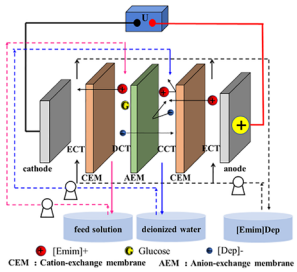

Figure 1: Scheme of ED stack used in this study.

2.4. Membrane Cleaning Experiments

Several cleaning solutions, such as high-quality rinse-water, alkali, acids, and surfactants, were regularly or even daily employed to wash membranes in industries to reduce the impacts of membrane foulants [30]. In this work, three kinds of solutions, i.e., ultra-pure water, hydrochloride solution, and sodium hydroxide solution, were selected as the cleaning solutions. A number of membrane samples of 40 mm × 40 mm were immersed in 100 mL of a cleaning solution (ultra-pure water, 0.1 mol/L HCl solution, or 0.1 mol/L NaOH solution) in an Erlenmeyer. Subsequently, each sample removed from the solution after a specified cleaning duration (1, 2, 3, 4, 5 day-D_1, D_2, D_3, D_4, D_5), was rinsed in 100 mL ultra-pure water for 24 h, and then was air-dried for further characterization.

2.5. Characterizations

The zeta potential of mixed solution containing IL and glucose was measured by Nanoparticle size and Zeta potential analyzer (DelsaNano C, Beckman Coulter, USA). ^{1}H and ^{13}C NMR spectra were recorded on a 600 MHz liquid NMR spectrometer (AVANCE III HD 600, Bruker, Switzerland). The surface structure of the IEMs was characterized by Fourier Transform Infrared spectrophotometer (FT-IR) (Nicolet 380, Thermo Nicolet Corporation, USA) from 4000 to 600 cm^{-1} and X-ray photoelectron spectrometer (XPS). The surface morphology of IEMs was observed by SEM (Hitachi SU8020, Japan) at an accelerating voltage of 5 kV and a current of 10 μA. EDS was used to obtain the surface and cross-section element mapping of IEMs at an accelerating voltage of 20 kV and a current of 10 μA. The roughness of the surface of the IEMs was determined by atomic force microscopy (AFM) (MultiMode 8, Bruker, Germany). The elemental content of the CEM was analyzed by elemental analyzer (vario EL cube, Elementar Analysensysteme GmbH, Germany). The surface contact angle of IEMs was determined by contact angle instrument (K100, Kruss, Germany).

The IEC of IEMs was determined by titration [31]. The determination steps of IEC of AEM are as follows: the AEM with the size of 30 mm × 30 mm was weighed as m_b (g), and then the AEM with known weight was immersed in the 20 mL of 0.1 mol/L NaOH solution for 24 h to ensure that all the opposite ions were converted into OH^-. Subsequently, the NaOH solution was titrated with the 0.01 mol/L HCl solution. The volume of HCl solution was recorded as V_b (mL), and the IEC of AEM can be obtained by Eq. (1). The determination method of IEC for CEM was the same as that of AEM. The difference was that the CEM was immersed in the 0.1 mol/L HCl solution, and the HCl solution was titrated with the 0.01 mol/L NaOH solution.

3. Results and Discussions

3.1. Determination of Limit Current Density

When the current density reaches the limit current density (LCD), H_2O molecules on the membrane's surface are dissociated into H^+ and OH^- ions, causing membrane fouling to worsen. As a result, the LCD value is a critical parameter for the ED process, and it can be calculated using the current density and potential relationship [32,33]. The LCD parameter was tuned in this study by looking at the applied voltage drop across the membrane stack. The experiment was conducted with a 2 L dilute solution (10 g/L IL and 0.5 g/L glucose), a 2 L concentrated solution (distilled water), and a 40 L/h flow rate. The changing patterns of the current density during the ED process as the voltage declines were depicted in **Figure 2**. The slope was clearly modified due to H_2O dissociation on the membrane surface, and the LCD was then around 1.73 mA/cm^2, which was employed in the subsequent ED studies.

3.2. Zeta Potential of IL and Glucose in a Mixed Solution

Zeta potential is another important parameter to control the electrostatic interaction between organic compounds and membranes [12]. **Figure 3** shows the zeta potential variation of a mixed solution containing IL and glucose as a function of [Emim]Dep and glucose concentrations. It was obvious from **Figure 3(a)** that the surface potential of the mixed solution was negative and its absolute value increased with the increase of [Emim]Dep concentration. From **Figure 3(b)**, it was clear that the absolute value of surface potential decreased with the increase of glucose concentration. This might be attributed to the fact that glucose was easier to adhere to the surface of CEM. Therefore, it was speculated that the higher the concentration of glucose in the feed solution, the more serious the fouling of CEM would be [34].

3.3. Analysis of Fouling for IEMs

To reduce the effect of concentration polarization on membrane fouling, the experimental current density should be controlled below the LCD. From the above experimental results, the applied voltage corresponding to the LCD was 7.64 V. As a result, the applied voltage of 6 V was chosen for further studies based on LCD requirements.

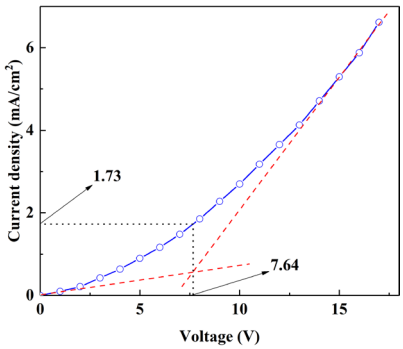

Figure 2: The current density and potential relationship.

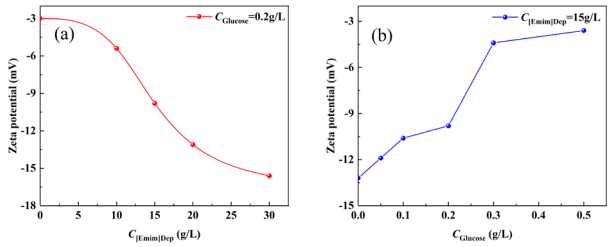

Figure 3: Zeta potential Variation of the mixed solution containing IL and glucose with the concentration of [Emim]Dep **(a)**, glucose**(b)**.

3.3.1. Effect of the Operating Time on Membrane Fouling

The effect of operation time on membrane fouling was evaluated in this study using a 2 L dilute solution (30 g/L IL and 0.2 g/L glucose), a 2 L concentrated solution (distilled water), a 6 V applied voltage, a 25 °C dilute solution temperature, and a 40 L/h flow rate. The IEC of fouled membranes is listed in **Table 2**. It was obvious that the IECs for both AEMs and CEMs decreased with the increasing operating time. When the operating time was increased from 0 to 4 h, the IEC of IEMs was obviously decreased. A further increase of operating time from 4 h, caused a slight change for the IEC of IEMs. It might be due to the fact that a large amount of [Emim]Dep in the DCT were transferred into the CCT during the initial stage of ED process. The variance of the permeation ratio for IL with the operating time has been investigated in our previous study **[11]**. It was found that in the first third of the whole separation process, nearly half of [Emim]Dep in the DCT were transferred through the IEMs to the CCT. Moreover, the time required for the complete transfer of [Emim]Dep to the CCT in this condition experiment was about 8 h. Therefore, in the first 4 h, most of [Emim]Dep in the DCT were transferred to the CCT through the IEMs, leading to deterioration of the IEC due to the internal blockage of IEMs. In addition, it can also be found from **Table 2** that the IEC of CEMs decreased faster than that of AEMs, due to the fact that glucoses was easy to be enriched on the surface of the CEM, which might promote the formation of IL clusters on the surface of the CEM, and further lead to the blockage of ILs in the membrane pores or interlayers, thus accelerating the membrane fouling.

Contact angle is an important parameter to characterize the hydrophilicity of membrane surface. The results of contact angle measurements for the fouled IEMs at different operating time are shown in **Figure 4**. The pristine IEMs used in this study were hydrophobic due to the fact that contact angles for these membranes were higher than 90°. The surface contact angles of AEMs and CEMs decreased with the extension of operation time, indicating that the membrane surface became less hydrophobic due to the adsorption of [Emim]Dep or glucose. It needs to be mentioned that, as shown in **Figure 4**, when the operation time increased from 0 h to 4 h, the surface contact angles of CEM and AEM showed a slight change. But with the further increase of the operating time from 4 h to 6 h, the contact angle of membrane surface decreased obviously. However, when the operating time increased from 6 h to 8 h, the contact angle showed no obvious change. This could be due to the fact that the amount of [Emim]Dep adsorbed on the surface of IEMs gradually reached the maximum with the extension of operating time.

Figure 5 shows the surface morphologies of pristine IEMs and different fouled IEMs. It was shown that the surface morphology of contaminated AEMs had changed in some way. The longer the operating time, the more obvious the changes of surface morphology. As shown in **Figure 5(b)**, the surface morphology of AEM was similar to **Figure 5(a)**, but the ILs were found on the surface of AEM. In addition, it was clear from **Figure 5(c)** to **Figure 5(e)** that the surface morphology of fouled AEMs was completely different from that of pristine AEM, due to the formation of dense fouling layer.

It can also be seen from **Figure 5** that the surface morphology of CEM only happened a slight change. However, according to the changes of IEC and surface contact angle, it can be found that the extension of operating time also increased the fouling degree of CEM. No obvious change in morphology might be due to the fact that the surface morphology of pollutants is similar to that of pristine CEM. The surface roughness of pristine and fouled IEMs were examined to further validate the fouling of IEMs. The results are shown in **Figure 6**. As can be observed from this figure, the surface roughness of all the fouled IEMs at different operating time increased, further indicating that the surface of IEMs was fouled.

Table 2: IECs of fouled membranes at different operating times.

Time (h)	IEC (mol/kg)	
	CEM	AEM
0	0.8663	0.5721
2	0.6535	0.5156
4	0.5625	0.4751
6	0.5370	0.4565
8	0.5082	0.4011

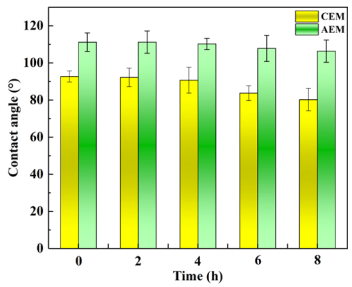

Figure 4: Contact angles on CEMs and AEMs at different operating time.

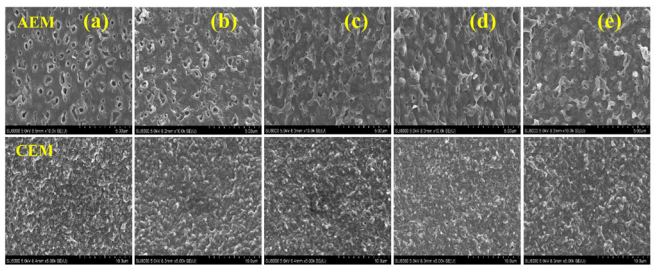

Figure 5: SEM images of the fouled AEMs and CEMs (a to e are 0, 2, 4, 6, 8 h).

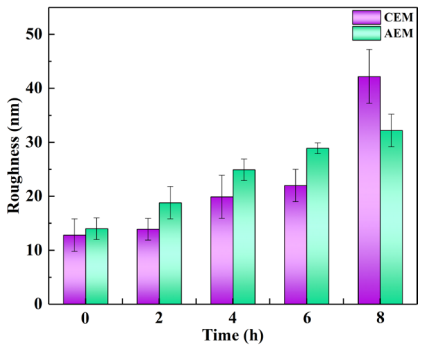

Figure 6: Roughness of CEMs and AEMs at different operating time.

The XPS spectra for IEMs were analyzed to elucidate the mechanisms, as shown in **Figure 7**. It can be seen from **Figure 7(a)** that the surface of pristine AEM mainly contained C, O, and F elements, and that of fouled AEM was still dominated by C, O, and F elements, but a new peak of P2p. The adsorption of Dep^- anion on the surface of fouling AEM was thought to be the origin of the alterations in chemical structure. It also was obvious from **Figure 7(b)** that the surface of pristine CEM mainly contained C, O, and F elements, and that of fouled CEM was still dominated by C, O, and F elements except for a new peak of N1s. This could be due to the fact that $[Emim]^+$ cation was adsorbed on the surface of CEM.

The change of chemical bond on the surface of AEM was further analyzed by the peak fitting function of XPSPEAK 4.0. **Figure 8(a)** and **Figure 8(b)** gave the fitting results of O1s peak. O1s was divided into six peaks, N-O, C-O, H-O, C=O/P-O, H-O, and C-O-C, with values of 530.57, 531.04, 531.50, 531.96, 532.44, and 533.10 eV, respectively. **Figure 8(c)** shows the peak fitting results of P2p. As shown in this figure, P2p was divided into two peaks, i.e. P-O and P=O, and their values were 133.07 and 133.92 eV, respectively, corresponding to Dep^- anion.

Similarly, the peak fitting function of XPSPEAK 4.0 was used to analyze the change of chemical bonds on the surface of CEM. **Figure 9(a)** and **Figure 9(b)** gave the results of O1s peak fitting. O1s was divided into four peaks, $-SO_3H$, C=O, C-O, and C-OH, with peaks of 531.11, 531.67, 532.31, and 533.10 eV, respectively. **Figure 9(c)** and **Figure 9(d)** show the fitting results of N1s peak. N1s was divided into three peaks, C-N, H-N, and $C-N^+$, and the corresponding values were 399.70 eV, 400.14 eV, and 401.50 eV, respectively. It also can be seen that the pristine CEM was dominated by H-N and C-N peaks. H-N peak accounted for the largest proportion. While the $C-N^+$ peak ratio of CEM increased significantly after fouling. It was inferred that the changes in the chemical bond of fouled CEM surface were caused by the adsorption of $[Emim]^+$ cation. In addition, it was also obvious from **Figure 9(a)** and **Figure 9(b)** that the ratio of C-OH peak for CEMs increased from 0% to 8.95% after fouling. It is speculated that glucoses could be adsorbed on the surface of CEM.

The operating time of 6 h was chosen for future studies in order to better understand the fouling mechanisms of IEMs, and based on the results of the impacts of operating time on membrane fouling.

3.3.2. Effect of the IL Concentration on Membrane Fouling

At a dilute solution of 2 L (0 g/L glucose), a concentrated solution of 2 L (distilled water), an applied voltage of 6 V, a dilute solution temperature of 25 °C, and a flow rate of 40 L/h, the influence of IL concentration on membrane fouling was examined. It can be seen from Supporting Information Table S1 that the IECs of CEMs and AEMs decreased from 0.8663 mol/L and 0.5721mol/L to 0.5720 mol/L and 0.4905 mol/L, respectively, when the initial IL concentration in the DCT increased from 0 to 10 g/L, indicating that the IL concentration had a great influence on the IEC of CEMs. This might be due to the fact that glucoses was easier to adhere to the surface of the CEM based on the results obtained in section 3.2, which promoted the clustering of ILs on the surface of the CEM and intensified the blockage of CEMs. With the further increase of IL concentration from 10 to 40 g/L, the IECs of AEMs and CEMs showed a slight change, indicating that the adsorption capacity of ILs on the AEMs reached a maximum value.

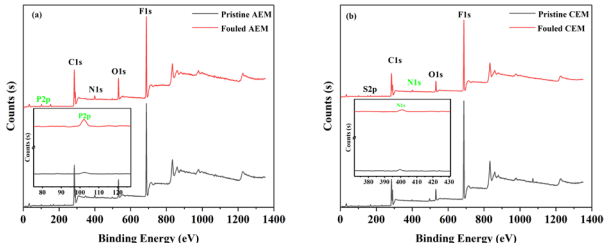

Figure 7: XPS spectra of AEMs **(a)** and CEMs **(b)** before and after fouled (t = 6 h; 30 g/L IL; 0.5 g/L glucose).

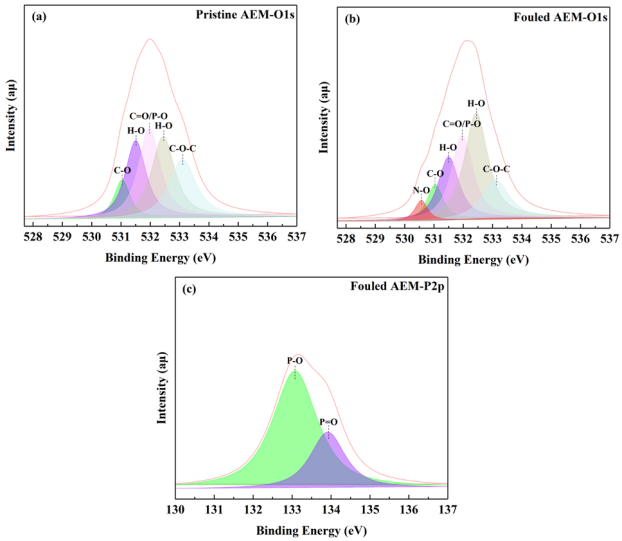

Figure 8: Sub-peak fitting diagram of O1s for the pristine AEM **(a)**, the fouled AEM **(b)** and P2p for the fouled AEM **(c)**.

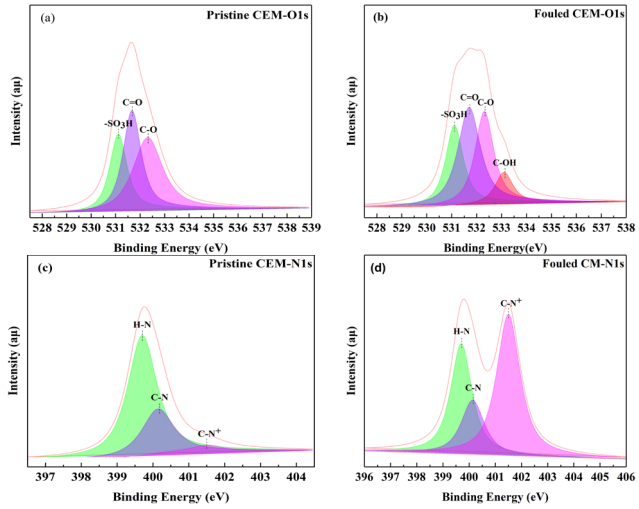

Figure 9: Sub-peak fitting diagram of O1s for the pristine CEM **(a)**, the fouled CEM **(b)** and N1s for the pristine CEM **(c)** and the fouled CEM **(d)**.

In order to further explain the phenomenon, the elemental content of the fouled membrane was analyzed. It was obvious from **Figure 10** that the P content for the fouled AEMs surface increased with the increase of IL concentration and hardly happened any changes for the fouled CEMs surface. However, it can be seen from **Figure 11** that the N content for the fouled CEMs obviously increased. This could be due to the fact that Dep^- anion and $[Emim]^+$ cation of the IL were adsorbed in AEMs and CEMs, respectively. In addition, it was obvious from **Figure 10** and **Figure 11** that the P content on the AEM and the N content on the CEM were 3.68% and 2.37% at the IL concentration of 10 g/L respectively. With the further increase of IL concentration, however, the changes in the P content on the surface of AEMs and the N content on the CEM were not obvious.

The contact angle of the fouled IEMs at different IL concentrations is shown in Supporting Information Figure S3. It was clear that when the concentration of IL increased, the contact angle of IEMs reduced, due to the fact that ILs were adsorbed on the surface of IEMs. However, IL investigated in this work was hydrophilicity, leading to a decrease for the hydrophobicity of the fouled membranes.

FT-IR spectra for the pristine IEMs and the fouled IEMs dried naturally were used to analyze the changes in chemical structure for the surface of the fouled IEMs. The results are shown in **Figure 12**. It can be seen from **Figure 12(a)** that, for the fouled CEMs, two new absorption peaks appeared at 1571 cm^{-1} and 1337 cm^{-1}, and their peak intensities increased with the increasing IL concentration. The two new peaks corresponded to C=N and C-N stretching vibration, respectively, which was consistent with the characteristic peak of $[Emim]^+$. Moreover, The characteristic peak of the S-O bond in the functional group sulfonic acid group of the cation exchange membrane shifted before and after the fouling, changing from 1036 cm^{-1} to 1030 cm^{-1}. This might be attributed to the adsorption of the $[Emim]^+$ on the surface of the CEM by electrostatic interaction.

For the AEMs, As shown in **Figure 12(b)**, it was obvious that two new absorption peaks appear at 1045 cm^{-1} and 943 cm^{-1} after the experiment of membrane fouling, and the peak intensity increased with the increase of IL concentration. The two new peaks corresponded to P=O and P-O stretching vibrations, respectively, which were consistent with the characteristic peaks of Dep^-. The characteristic peak of the C-N bond in the functional group quaternary ammonium group of the anion exchange membrane shifted before and after the fouling, changing from 1169 cm^{-1} to 1167 cm^{-1}. This could be due to the fact that Dep^- anions were adsorbed on the surface of AEM by electrostatic interaction. And the increase of IL concentration in the DCT led to an increase in the total amount of Dep^- anions absorbed on the AEM surface.

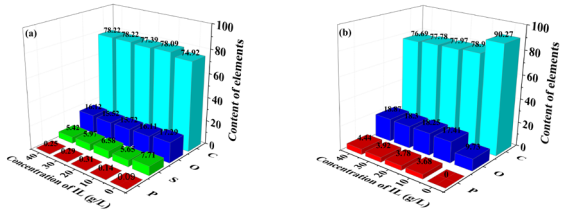

Figure 10: Variation of element content on the surface of fouled CEMs **(a)** and AEMs **(b)** by EDS analysis.

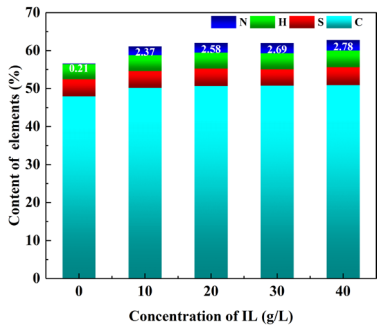

Figure 11: Elemental analysis of the fouled CEMs.

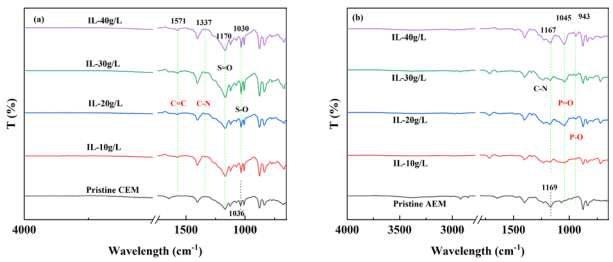

Figure 12: FT-IR spectra of CEMs **(a)** and AEMs **(b)** before and after fouled at different IL concentrations.

3.3.3. Effect of the Glucose Concentration on Membrane Fouling

Experiments were carried out using a dilute solution of 2 L (30 g/L IL), a concentrated solution of 2 L (distilled water), an applied voltage of 6 V, a dilute solution temperature of 25 °C, and a flow rate of 40 L/h to determine the influence of glucose concentration on the IEC of membrane. **Table 3** shows the results of the experiment.

As shown in **Table 3**, the glucose concentration hardly affected the IEC of the AEMs. However, the glucose concentration showed a certain influence on the IEC of CEMs. The IEC of CEMs declined from 0.5465 mol/kg to 0.4978 mol/kg during the glucose concentration range of 0 to 0.5 g/L. This might be due to the fact that glucose was easily adsorbed on the surface of CEMs. The interactions between 1-butyl-3-methylimidazolium carboxylate IL and glucose were investigated by Zhuo et al. [35]. The hydrogen bonds between H2 in the imidazolium ring and H_2O molecules were discovered to be weakened when glucose was added to the aqueous solution. The interaction between the IL anion and glucose was stronger than the interaction between the IL cation and glucose, and a small amount of glucose might produce a change in the aggregation characteristics of IL. As a result, the aggregations of glucose and IL on the surface of the CEMs increased as the glucose concentration increased. This caused a negative impact on the charged groups in the CEMs, and thus reducing the IEC of the CEM.

The glucose concentration hardly affected the contact angle of AEMs, but did have a slight effect on the contact angle of CEMs, as shown in **Figure 13**. The contact angle of CEMs declined from 82.93° to 77.27° during the glucose concentration range of 0 to 0.5 g/L. This might be since an increase in glucose concentration increased the aggregations between glucose and IL, thus further increased the adsorption contents of IL and glucose on the surface of the CEMs. Especially, the hydrophilic glucose and IL absorbed on the surface of CEMs reduced the hydrophobicity of membrane surface.

3.3.4. Effect of Temperature on Membrane Fouling

At a dilute solution of 2 L (30 g/L IL and 0.2 g/L glucose), a concentrated solution of 2 L (distilled water), a voltage of 6 V, and a flow rate of 40 L/h, the influence of temperature on membrane fouling was examined. Supporting Information Table S2 listed the IEC of the fouled membranes at different temperatures. It was obvious that the temperature had a great influence on the IEC of CEMs and AEMs. Over the temperature range from 25 to 40 °C, the IEC of CEMs and AEMs decreased from 0.5370 mol/kg and 0.4565 mol/kg to 0.4171 mol/kg and 0.3172 mol/kg, respectively.

Table 3: IECs of fouled membranes at different glucose concentration.

Concentration glucose (g/L)	IEC (mol/kg)	
	CEM	AEM
0	0.5465	0.4632
0.1	0.5377	0.4592
0.2	0.5370	0.4565
0.3	0.5164	0.4581
0.5	0.4978	0.4511

However, it can be found from **Figure 14** that with the increase of temperature, the contents of P element on the surface of AEMs and N element on the surface of CEMs showed slight changes. These findings showed that as the temperature increase, the degree of membrane fouling increase as well. Other researchers have also drawn the same conclusion **[36]**. They found that higher temperature led to the change of membrane structure and morphology, which had a negative impact on the charged groups in the IEMs, and thus decreased the IEC of IEMs.

3.4. Membrane Cleaning

3.4.1. Effect of the Type of Cleaning Solution on the Performance of Cleaning

Table 4 listed the IEC of the fouled membranes immersed in different cleaning solution. It can be seen that when the fouled CEMs were immersed in the distilled water, 0.1 mol/L HCl and 0.1 mol/L NaOH solutions, the IECs of the CEM were 0.5436 mol/kg, 0.8193 mol/kg, and 0.8287 mol kg, respectively. Compared with the distilled water, the cleaning effects of the NaOH and HCl solutions were better. The distilled water had a little cleaning effect on fouled AEMs and AEMs, indicating that the adsorption of IL on the membrane might be happened by the chemical interaction between IL and the IEM. In addition, the HCl solution showed the best cleaning effect for the fouled AEMs. This result might be attributed to the Hoffmann elimination reaction and nucleophilic substitution reaction of quaternary ammonium groups of AEM under alkaline conditions **[36]**.

The roughness of the pristine and cleaned IEMs were analyzed, as shown in **Figure 15**. It was obvious that the roughness of the fouled IEMs cleaned by the distilled water happened with little changes. The roughness values of the AEMs cleaned by the HCl and NaOH solutions were 13.6 nm and 14.5 nm, respectively, which were close to the roughness value of the pristine AEM (14.0 nm). This result indicated that almost all the foulants absorbed on the surface of the AEMs could be effectively removed by the cleaning of the HCl or NaOH solution.

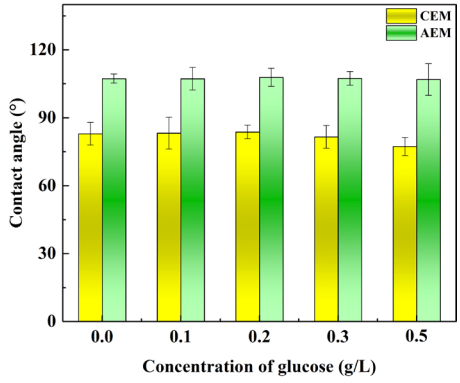

Figure 13: Contact angles on CEMs and AEMs at different glucose concentrations.

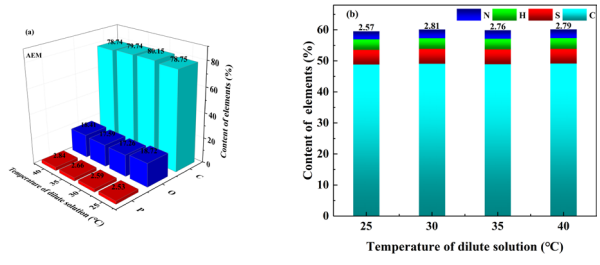

Figure 14: Variation of elements content of the surface of fouled AEMs by EDS analysis **(a)** and the fouled CEMs at different temperatures **(b)**.

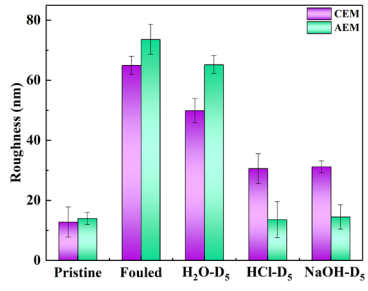

Figure 15: Roughness of the fouled membrane after immersion in different cleaning solutions.

Table 4: IECs of fouled membranes at different conditions.

Conditions	IEC (mol/kg)	
	CEM	AEM
Pristine	0.8663	0.5721
Fouled	0.5370	0.4565
H_2O-D_5	0.5436	0.4659
HCl-D_5	0.8193	0.5678
NaOH-D_5	0.8287	0.5382

It also can be found from **Figure 15** that the roughness values of the CEMs cleaned by the HCl and NaOH solutions were 30.6 nm and 31.2 nm, respectively, which were a little higher than that of the pristine CEM (12.8 nm). Most of the foulants adsorbed on the surface of CEMs could be removed by the cleaning of the HCl and NaOH solutions. The residual foulants on the CEM after cleaning had a certain influence on its surface morphology, resulting in the increase of the surface

roughness of the CEM. This result might be attributed to the intensification of IL clusters resulting in the blockage of CEM.

Based on the above experimental results, it can be seen that the cleaning effect of the distilled water was the worst. Therefore, taking into account the recovery of the performance of the fouled IEMs and the 0.1 mol/L HCl solution was selected as the cleaning solution for the subsequent experiments.

3.4.2. Effect of the Cleaning Time on the Performance of Cleaning

It can be seen from Supporting Information Table S3 that the IEC of CEMs could be recovered to 0.8260 mol/kg after one day of immersion. With the increase of cleaning time, the IEC of CEMs showed a slight change. The element analysis results for the CEMs were obtained by quantitative analysis test, as shown in **Figure 16**. It was obvious that after the fouled CEM was immersed in the HCl solution for one day, the content of N decreased from 2.78% to 0.79%. With the further increase of cleaning time, the content of N for the CEM happened almost no change, indicating that most of the foulants adsorbed on the CEMs could be removed by the method of immersion cleaning, and the CEM fouling was partially irreversible, due to the fact that ILs and glucoses blocked in the CEM pores or interlayers could not be effectively removed.

It can also be seen from Supporting Information Table S3 that the IEC of AEM was restored from 0.4565 mol/kg to 0.4769 mol/kg after the AEM was immersed in the HCl solution for one day. After five days of immersion, the IEC was 0.5678 mol/kg, slightly lower than that of the pristine AEM, indicating that the ILs adsorbed on the AEM could also be removed by the method of immersion cleaning. The element mapping of the fouled AEM immersed in the HCl solution for different time was shown in **Figure 17**. For the pristine AEM, the elements of C and O were evenly distributed on the membrane surface, and the P element should be the component of crosslinking agent for the synthesis of AEM. It also was obvious that the contents of O and P elements for the fouled AEM increased from 17.89% and 0.16% to 22.03% and 3.54%, respectively. When the immersion time of the fouled AEM was only one day (D_1), the contents of O and P elements changed slightly in comparison with the pristine AEM. It was analyzed that the immersion cleaning of one day caused a small part of foulants on the fouled AEM (D_0) to fall off and most of them to become loose. With the cleaning time increase to five days, the distribution of O and P elements (D_5) decreased significantly to 18.15% and 0.19%, respectively, indicating that the foulants on the surface of AEMs could be removed through the long-term immersion cleaning process.

In Supporting Information Figure S4, the element mapping on the cross-sections of the pristine and fouled AEMs immersed in the HCl solution for various times is displayed. It was obvious that the content of P element for the fouled AEM increased significantly, indicating that the anions of IL not only resulted in the fouling of AEM surface, but also blocked the pores or interlayers of AEM. In addition, with the extension of immersion time, the content of P element in the cross-section of AEM decreased gradually. When the AEM was immersed in the HCl solution for five days, the content of P element decreased from 1.47% to 0.19%, which was close to that of the pristine AEM. These results indicated that the Dep^- blocked in the membrane pores or interlayers could be removed by the cleaning method.

3.5. Analysis of IEM Fouling Mechanism

According to the results of membrane fouling and cleaning experiments, the fouling characteristics of the IEMs were significantly affected by ILs and glucoses interested in this work. **Figure 18** shows a schematic diagram of fouling behavior during ED removal of soluble saccharides from an aqueous solution containing ILs.

By comparing the cleaning effect of deionized water, hydrochloric acid, and sodium hydroxide solutions on the fouled membranes, it was found that the cleaning effect of deionized water on the AEM and CEM was worst, indicating that the foulants such as ILs and glucoses interacted with the IEMs not only by the physical adsorption, but also by the chemical reaction. This result could be confirmed by the XPS characterization results of the fouled membrane, which showed that a new N-O bond appeared on the surface of the AEM.

Combined with the analysis results of FTIR and XPS, it was obvious that anions and cations of ILs could be absorbed on the surface of AEMs and CEMs, respectively, by the electrostatic interactions due to the fact that the AEM contained positively charged quaternary ammonium groups and the CEMs contained negatively charged sulfonic acid groups. However, the IEC of the fouled membrane cannot be restored to the original value after a long time of cleaning, indicating that the fouling of the IEMs was partially irreversible, resulting from the blockage of ILs in the membrane pores or interlayers. Especially, the XPS characterization results of the fouled CEM showed that a new bond C-OH appeared on the surface of the fouled CEM, indicating that glucoses could be attached to the surface of the CEM. The experimental results indicated that the addition of glucose deteriorated the fouling level of the CEMs, due to the fact that glucoses was easy to be enriched on the surface of the CEM. This might promote the formation of IL clusters on the surface of the CEM, and further lead to the blockage of ILs in the membrane pores or interlayers.

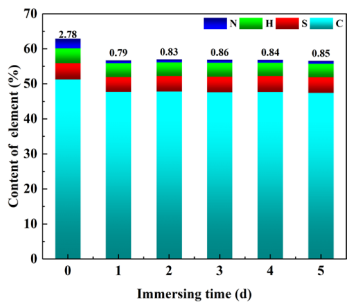

Figure 16: Elemental analysis of the fouled CEMs immersed in HCl for different time.

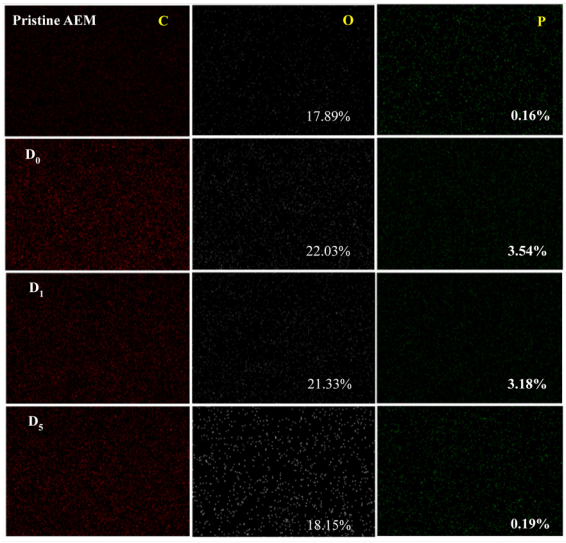

Figure 17: The element mapping for the pristine AEMs and the fouled AEMs.

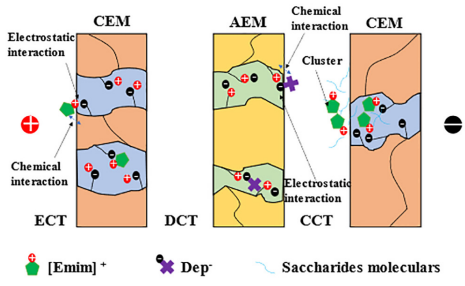

Figure 18: The schematic diagram of the fouling behavior during removal of soluble saccharides from the aqueous solution containing ILs by ED on the IEMs.

4. Conclusions

In this work, the IEM fouling was studied during the removal of soluble saccharides from the aqueous solution containing ionic liquids by the ED method. In order to study the effect of the ED process on the formation of IEMs fouling and property changes of the fouled IEMs, the experiments of IEMs fouling and cleaning were carried out. It was demonstrated that the low IL concentration also resulted in the fouling of the IEMs. The addition of glucose had a slight effect on the AEM, but a serious effect on the CEM. The effect of temperature on the IEM fouling was the most significant. Higher temperature resulted in the change of the IEM structure, and the IEC of the IEMs was significantly reduced with the increasing temperature. In addition, the hydrochloric acid solution showed a good cleaning effect for the fouled IEMs. A cleaning process of short time could recover the performance of the fouled CEMs to 94.57% of the pristine membrane, and that of the fouled AEMs could be returned to the pristine membrane level by a long cleaning process. During the ED process for the separation of glucoses from the IL aqueous solution, the IEM fouling was mainly caused by the adsorption of the anions and cations through electrostatic interactions. Glucoses was easier enriched on the surface of the CEMs, which could promote the cluster behavior of the IL, and then the blockage of ILs in the membrane pores or interlayers was intensified, further increasing the irreversible fouling of CEM.

Supplementary Materials

Figure S1 lists the ^{1}H NMR data of the synthesized [Emim]Dep IL. Figure S2 lists the ^{13}C NMR data of the synthesized [Emim]Dep IL. Figure S3 provides relationships between the contact angles of the IEMs and the IL concentrations. Figure S4 listing element content on the cross-section for the pristine and fouled AEMs. Table S1 lists the effect of IL concentration on the IECs of the fouled IEMs. Table S2 lists the effect of the temperature of dilute solutions on the IECs of the fouled IEMs. Table S3 lists the effect of the HCl cleaning solution on the IECs of the fouled IEMs.

Authors' Contributions

The paper was written through the contributions of all authors. All authors have approved the final version of the paper. Hongxiang Xu designed the experiments and revised the paper. Weichao Li executed experiments and wrote the paper. Wentao Li, Shanshan Zhang, Daoguang Wang, and Yi Nie gave some good suggestions about the experiments. Junfeng Wang guided the project and revised the paper.

Data Availability

The data supporting the findings of this study are available within the article and the supplementary materials.

Conflicts of Interest

The authors declare that there is no conflicts of interest.

Funding

This work was supported by the National Natural Science Foundation of China (21978302, U20A20149), Innovation Academy for Green Manufacture, Chinese Academy of Sciences (IAGM2020DB05), China Postdoctoral Science Foundation (NO. 2020M673551XB), Fundamental Research Funds for the Central Universities (NO. 2020QN08, NO. 2021YJSHH29).

References

[1] Li Y, Liu X, Zhang S, Yao Y, Yao X, Xu J, et al. Dissolving process of a cellulose bunch in ionic liquids: a molecular dynamics study. Phys Chem Chem Phys 2015;17:17894–905. https://doi.org/10.1039/C5CP02009C.

[2] Xu K, Xiao Y, Cao Y, Peng S, Fan M, Wang K. Dissolution of cellulose in 1-allyl-3-methylimidazolium methyl phosphonate ionic liquid and its composite system with Na2PHO3. Carbohydr Polym 2019;209:382–8. https://doi.org/10.1016/j.carbpol.2018.12.040.

[3] Brehm M, Pulst M, Kressler J, Sebastiani D. Triazolium-Based Ionic Liquids: A Novel Class of Cellulose Solvents. J Phys Chem B 2019;123:3994–4003. https://doi.org/10.1021/acs.jpcb.8b12082.

[4] Swatloski RP, Spear SK, Holbrey JD, Rogers RD. Dissolution of Cellose with Ionic Liquids. J Am Chem Soc 2002;124:4974–5. https://doi.org/10.1021/ja025790m.

[5] Yang J, Lu X, Zhang Y, Xu J, Yang Y, Zhou Q. A facile ionic liquid approach to prepare cellulose fiber with good mechanical properties directly from corn stalks. Green Energy

& Environment 2020;5:223–31. https://doi.org/10.1016/j.gee.2019.12.004.

[6] Zhang Y, Bakshi BR, Demessie ES. Life Cycle Assessment of an Ionic Liquid versus Molecular Solvents and Their Applications. Environ Sci Technol 2008;42:1724–30. https://doi.org/10.1021/es0713983.

[7] Xu A, Wang J, Wang H. Effects of anionic structure and lithium salts addition on the dissolution of cellulose in 1-butyl-3-methylimidazolium-based ionic liquid solvent systems. Green Chem 2010;12:268–75. https://doi.org/10.1039/B916882F.

[8] Nie Y, Li C, Sun A, Meng H, Wang Z. Extractive Desulfurization of Gasoline Using Imidazolium-Based Phosphoric Ionic Liquids. Energy Fuels 2006;20:2083–7. https://doi.org/10.1021/ef060170i.

[9] Kamiya N, Matsushita Y, Hanaki M, Nakashima K, Narita M, Goto M, et al. Enzymatic in situ saccharification of cellulose in aqueous-ionic liquid media. Biotechnol Lett 2008;30:1037–40. https://doi.org/10.1007/s10529-008-9638-0.

[10] Falca G, Musteata V-E, Behzad AR, Chisca S, Nunes SP. Cellulose hollow fibers for organic resistant nanofiltration. Journal of Membrane Science 2019;586:151–61. https://doi.org/10.1016/j.memsci.2019.05.009.

[11] Li W, Wang J, Nie Y, Wang D, Xu H, Zhang S. Separation of soluble saccharides from the aqueous solution containing ionic liquids by electrodialysis. Separation and Purification Technology 2020;251:117402. https://doi.org/10.1016/j.seppur.2020.117402.

[12] Zhao Z, Shi S, Cao H, Li Y, Van der Bruggen B. Comparative studies on fouling of homogeneous anion exchange membranes by different structured organics in electrodialysis. Journal of Environmental Sciences 2019;77:218–28. https://doi.org/10.1016/j.jes.2018.07.018.

[13] Lee H-J, Choi J-H, Cho J, Moon S-H. Characterization of anion exchange membranes fouled with humate during electrodialysis. Journal of Membrane Science 2002;203:115–26. https://doi.org/10.1016/S0376-7388(01)00792-X.

[14] Lee H-J, Hong M-K, Han S-D, Shim J, Moon S-H. Analysis of fouling potential in the electrodialysis process in the presence of an anionic surfactant foulant. Journal of Membrane Science 2008;325:719–26. https://doi.org/10.1016/j.memsci.2008.08.045.

[15] Xia Q, Qiu L, Yu S, Yang H, Li L, Ye Y, et al. Effects of Alkaline Cleaning on the Conversion and Transformation of Functional Groups on Ion-Exchange Membranes in Polymer-Flooding Wastewater Treatment: Desalination Performance, Fouling Behavior, and Mechanism. Environ Sci Technol 2019;53:14430–40. https://doi.org/10.1021/acs.est.9b05815.

[16] Bukhovets A, Eliseeva T, Oren Y. Fouling of anion-exchange membranes in electrodialysis of aromatic amino acid solution. Journal of Membrane Science 2010;364:339–43. https://doi.org/10.1016/j.memsci.2010.08.030.

[17] Tanaka N, Nagase M, Higa M. Organic fouling behavior of commercially available hydrocarbon-based anion-exchange membranes by various organic-fouling substances. Desalination 2012;296:81–6. https://doi.org/10.1016/j.desal.2012.04.010.

[18] Guo H, Xiao L, Yu S, Yang H, Hu J, Liu G, et al. Analysis of anion exchange membrane fouling mechanism caused by anion polyacrylamide in electrodialysis. Desalination 2014;346:46–53. https://doi.org/10.1016/j.desal.2014.05.010.

[19] Thompson DW, Tremblay AY. Fouling in steady and unsteady state electrodialysis. Desalination 1983;47:181–8. https://doi.org/10.1016/0011-9164(83)87071-4.

[20] Bleha M, Tishchenko G, Šumberová V, Kůdela V. Characteristic of the critical state of membranes in ED-desalination of milk whey. Desalination 1992;86:173–86. https://doi.org/10.1016/0011-9164(92)80032-5.

[21] Bailly M, Roux-de Balmann H, Aimar P, Lutin F, Cheryan M. Production processes of fermented organic acids targeted around membrane operations: design of the concentration step by conventional electrodialysis. Journal of Membrane Science 2001;191:129–42. https://doi.org/10.1016/S0376-7388(01)00459-8.

[22] Hábová V, Melzoch K, Rychtera M, Sekavová B. Electrodialysis as a useful technique for lactic acid separation from a model solution and a fermentation broth. Desalination 2004;162:361–72. https://doi.org/10.1016/S0011-9164(04)00070-0.

[23] Grossman G, Sonin AA. Membrane fouling in electrodialysis: a model and experiments. Desalination 1973;12:107–25. https://doi.org/10.1016/S0011-9164(00)80178-2.

[24] Grossman G, Sonin AA. Experimental study of the effects of hydrodynamics and membrane fouling in electrodialysis. Desalination 1972;10:157–80. https://doi.org/10.1016/S0011-9164(00)80084-3.

[25] Mulyati S, Takagi R, Fujii A, Ohmukai Y, Matsuyama H. Simultaneous improvement of the monovalent anion selectivity and antifouling properties of an anion exchange membrane in an electrodialysis process, using polyelectrolyte multilayer deposition. Journal of Membrane Science 2013;431:113–20. https://doi.org/10.1016/j.memsci.2012.12.022.

[26] Mulyati S, Takagi R, Fujii A, Ohmukai Y, Maruyama T, Matsuyama H. Improvement of the antifouling potential of an anion exchange membrane by surface modification with a polyelectrolyte for an electrodialysis process. Journal of Membrane Science 2012;417–418:137–43. https://doi.org/10.1016/j.memsci.2012.06.024.

[27] Bdiri M, Dammak L, Larchet C, Hellal F, Porozhnyy M, Nevakshenova E, et al. Characterization and cleaning of anion-exchange membranes used in electrodialysis of polyphenol-containing food industry solutions; comparison with cation-exchange membranes. Separation and Purification Technology 2019;210:636–50. https://doi.org/10.1016/j.seppur.2018.08.044.

[28] Bdiri M, Dammak L, Chaabane L, Larchet C, Hellal F, Nikonenko V, et al. Cleaning of cation-exchange membranes used in electrodialysis for food industry by chemical solutions. Separation and Purification Technology 2018;199:114–23. https://doi.org/10.1016/j.seppur.2018.01.056.

[29] Ghalloussi R, Garcia-Vasquez W, Chaabane L, Dammak L, Larchet C, Deabate SV, et al. Ageing of ion-exchange membranes in electrodialysis: A structural and physicochemical investigation. Journal of Membrane Science 2013;436:68–78. https://doi.org/10.1016/j.memsci.2013.02.011.

[30] Strathmann H, editor. Ion-Exchange Membrane Separation Processes. vol. 9. Elsevier B.V.; 2004.

[31] Chen S-S, Li C-W, Hsu H-D, Lee P-C, Chang Y-M, Yang C-H. Concentration and purification of chromate from electroplating wastewater by two-stage electrodialysis

processes. J Hazard Mater 2009;161:1075–80. https://doi.org/10.1016/j.jhazmat.2008.04.106.

[32] Lee H-J, Strathmann H, Moon S-H. Determination of the limiting current density in electrodialysis desalination as an empirical function of linear velocity. Desalination 2006;190:43–50. https://doi.org/10.1016/j.desal.2005.08.004.

[33] Cheng G, Wang Q, Sun X, Meng H, Li J. Experimental study on concentration of ammonium lactate solution from kitchen garbage fermentation broth by two-compartment electrodialysis. Separation and Purification Technology 2008;62:205–11. https://doi.org/10.1016/j.seppur.2008.01.015.

[34] Zhao Z, Shi S, Cao H, Li Y. Electrochemical impedance spectroscopy and surface properties characterization of anion exchange membrane fouled by sodium dodecyl sulfate. Journal of Membrane Science 2017;530:220–31. https://doi.org/10.1016/j.memsci.2017.02.037.

[35] Zhuo K, Chen Y, Chen J, Bai G, Wang J. Interactions of 1-butyl-3-methylimidazolium carboxylate ionic liquids with glucose in water: a study of volumetric properties, viscosity, conductivity and NMR. Phys Chem Chem Phys 2011;13:14542–9. https://doi.org/10.1039/C1CP20948E.

[36] Garcia-Vasquez W, Dammak L, Larchet C, Nikonenko V, Grande D. Effects of acid–base cleaning procedure on structure and properties of anion-exchange membranes used in electrodialysis. Journal of Membrane Science 2016;507:12–23. https://doi.org/10.1016/j.memsci.2016.02.006.

How to Cite

Xu H, Li W, Wang J, Li W, Zhang S, Nie Y, et al. Study on Fouling Mechanisms of Homogeneous Ion-Exchange Membranes during Removal of Soluble Saccharides from the Aqueous Solution Containing Ionic Liquids by Electrodialysis. Membrane Sci Int 2022;1(1):12–23.